

# Analysis of Material Optimization and Performance Parameter Difference of Expandable Sand Screen

Xinyuan WU\*, Junchi LIN\*, Hao TIAN\*, Wenling YANG\*\*, Yue WANG\*\*

\*Mechanical Engineering College, SiChuan University of Science & Engineering, 644005 Yibin, China,  
E-mail: wuxinyuan@suse.edu.cn (Corresponding Author)

\*\*CNPC Bohai Drilling Engineering Company Limited, 300280 Tianjin, China

<https://doi.org/10.5755/j02.mech.39559>

## 1. Introduction

The oil reservoirs situated in the unconsolidated sandstone represent a significant component of China's oil and gas resources, the extensive distribution and substantial reserves of these reservoirs provide a robust foundation for China's energy security [1].

The loose sandstone reservoirs are prone to sand production, which seriously affects production and leads to a decline in output, equipment damage, even well instability, and eventually may cause the oil well to be scrapped. Continuous exploitation will continuously deplete the reservoir energy, causing more sand to enter the production pipeline and exacerbating the sand production problem in the oil wells [2].

The expandable sand screen has a number of unique advantages. First, it offers a large inflow area that minimizes screen plugging and erosion. Second, it is operationally simple to install. Third, it offers a larger internal diameter than most sand-control screens, thus facilitating tubular installation for zonal isolation. Fourth, in open hole applications, an expandable sand screen eliminates the annulus between the screen and the sand face. This provides additional advantages in terms of sand control, increased production, and cost reduction [3], which has led to the fact that this technology has been widely used in oilfields.

Depending on the operating environment of the expandable sand screen, higher performance of the base tube material of the expandable sand screen is required. The material properties of the base pipe need to meet the following criteria: 1. No tearing or other conditions that may cause expansion failure are present during the expansion process; 2. It is imperative that the maximum expansion force applied during the construction of the expandable sand screen is as minimal as possible in order to reduce the expansion force requirements on the construction equipment. In order to satisfy the aforementioned two requirements, the base tube material must possess the requisite strength, hardness, plasticity, toughness and fracture toughness in order to minimize deformation and thus ensure the longest possible working life [4]. Furthermore, the corrosion and erosion resistance, and high temperature stability of the expandable sand screen are subject to varying requirements depending on the different operating conditions to which they are subjected throughout their lifetime. Considering the various requirements for the use of expandable sand screen materials, materials with good physical properties (including plasticity, toughness and fracture toughness, etc.) should be selected to ensure that the materials have adequate strength and good hardening effect.

The development of sand prevention technology of expandable sand screen is strictly limited by the performance of base tube material, and the selection of suitable material is one of the key influencing factors to make the progress of sand prevention technology of expandable sand screen. In order to accelerate the development of sand prevention technology of expandable sand screen, many scholars at home and abroad have carried out a lot of research on the material of expandable sand screen. Omar S. Al-Abri et al. analyzed the change rule of mechanical properties of the expansion sand screen by studying the change of the microstructure of the expansion tube during the expansion process, which was helpful to optimize the material design [5]. Dejun Li et al. examined the alterations in corrosion resistance prior to and following the 20G expansion, utilizing corrosion of expanded solid tubing in simulated fluids of varying oil well produced water, it will be helpful to guide the thread test and overall performance test of the expansion sand screen and lay a technical foundation for the further research of the expansion sand screen [6]. Yifeng Zhang et al. compared the differences in Anti-extrusion damage strength between TRIP and 20G after expansion based on the Bauschinger effect and residual stresses [7]. Jingjing Chen et al. developed an expansion force calculation model through a combination of material experiments and expansion experiments, and investigated the impact of material properties on expansion force [8].

In the field of expandable sand screen materials research, Scholars usually explore from multiple dimensions, including the modification techniques employed for the materials in question, the impact of microstructure on the functionality of expansion sand screen, and the influence of the Bauschinger effect and residual stress. Nevertheless, the majority of these studies are founded upon a substantial corpus of material experiments and test results. The undertaking of such studies demands a considerable investment of time and resources, and is further characterized by the presence of considerable economic costs and a relatively intricate staff structure. This paper employs a combination of material tensile testing, full-scale prototype expansion testing, and finite element analysis to identify the key factors influencing the tearing phenomenon observed during the expansion of the base tube. The theoretical basis is taken into account throughout the process, with a particular focus on the comparison and analysis of the experimental results obtained from five distinct materials. This study employs a combination of experimental data and theoretical analyses with the objective of identifying reference indicators that can be used to assess the risk of tearing phenomena in materials during expansion.

The comparative finite element analysis results are used to evaluate the expansibility of different materials in the manufacture of expandable sand screen. It is hoped that this paper will provide a theoretical reference basis for the selection of materials for expandable sand screen, thereby saving part of the research cost.

## 2. Base Tube Expansion Analysis

If the structural parameters and materials of the expandable sand screen are not properly selected, it will cause the base tube to tear during the expansion process, resulting in expansion failure, and the tearing phenomenon of the expandable sand screen is shown in Fig. 1 [9].

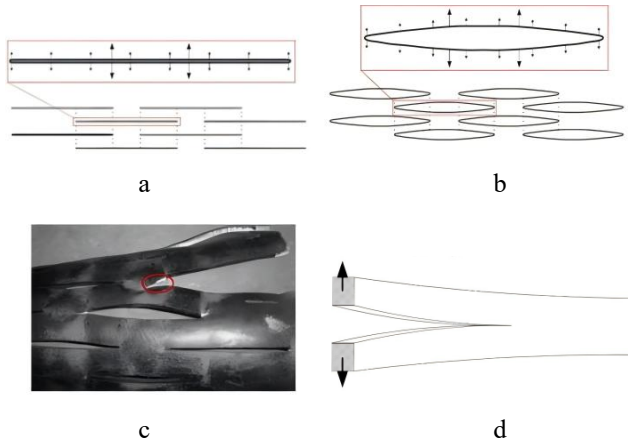


Fig. 1 Schematic diagram of base tube stress and failure: a – schematic diagram of the force on the kerf before expansion, b – schematic diagram of the force on the kerf after expansion, c – tearing of base tube, d – type I open

As shown in Fig. 1, the force deformation of the expandable sand screen is similar to that of the type I open crack. And the width of the kerf is so different from the diameter of the expandable sand screen that it can be analyzed by referring to the crack expansion part of fracture mechanics and considering the kerf as a crack subjected to load.

In fracture mechanics [10], the material aspect is mainly by the fracture toughness of the material, material defects and microcracks and other aspects as an index to measure the tearing resistance of the expandable sand screen; the structural aspect is mainly by the structural characteristics, subject to load mode and other aspects as an index to measure the tearing resistance of the expandable sand screen. Therefore, in addition to choosing reasonable parameters of the kerf structure of the expandable sand screen to alleviate the stress concentration of the base tube, by choosing reasonable materials of the expandable sand screen, it can also effectively improve the ability of the base tube to resist tearing and increase the expansibility of the expandable sand screen.

The material and organization of the expandable sand screen can effectively enhance the tear resistance of the base tube. However, due to the complexity of the operating conditions of the expandable sand screen, it is extremely difficult to analyze the stress distribution at the end of the base tube by theory. Therefore, the finite element method was used to differentially analyze the stress situation at the end of the kerf of expandable sand screens of different materials.

## 3. Expansion Experiment

### 3.1. Selection of Materials

According to the plasticity, strength and pitting resistance equivalent of the material, five materials, 654SMo, Incoloy 27-7Mo, 2507, Incoloy 625 and 316L, are selected to produce full-size prototype and tensile test specimens of the expandable sand screen. The comparison and analysis of the differences between the experimental results of the five materials, by consulting relevant literature [11, 12], the material properties of the five materials are shown in Table 1.

Table 1

Material properties of the five

Materials	654 SMO	Incoloy 27-7Mo	2507	Incoloy 625	316L
Yield strength, MPa	430	414	750	500	353
Tensile strength, MPa	855	827	879	960	663
Elongation, %	21.4	50.8	21.7	59.5	60
PREN, 1	55.94	46.09	42.66	52.23	24.13

Five materials yield strength from high to low for: 2507, Incoloy 625, 654SMo, Incoloy 27-7Mo, 316L; tensile strength from high to low for: Incoloy 625, 2507, 654SMo, Incoloy 27-7Mo, 316L; elongation from high to low for: 316L, Incoloy 625, Incoloy 27-7Mo, 2507, 654SMo; pitting resistance equivalent from high to low: 654SMo, Incoloy 625, Incoloy 27-7Mo, 2507, 316L.

Tensile tests at room temperature were conducted in accordance with the standard GB/T 228.1-2021 (ambient temperature of the laboratory at 10°C), as shown in Fig. 2. Five types of material tensile test specimens were processed. Fig. 3 shows the tensile test of the specimens. The testing equipment was a microcomputer-controlled electronic universal testing machine YSLX-02UTM5305SYXL.

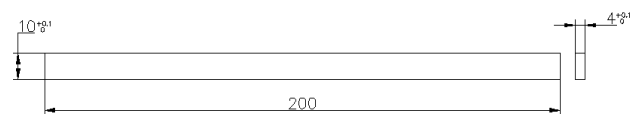


Fig. 2 Samples of tensile tests



Fig. 3 Specimen tensile test

### 3.2. Analysis of material tensile experiment results

Fig. 4 illustrates the condition of the experimental samples of diverse materials following tensile fracture.

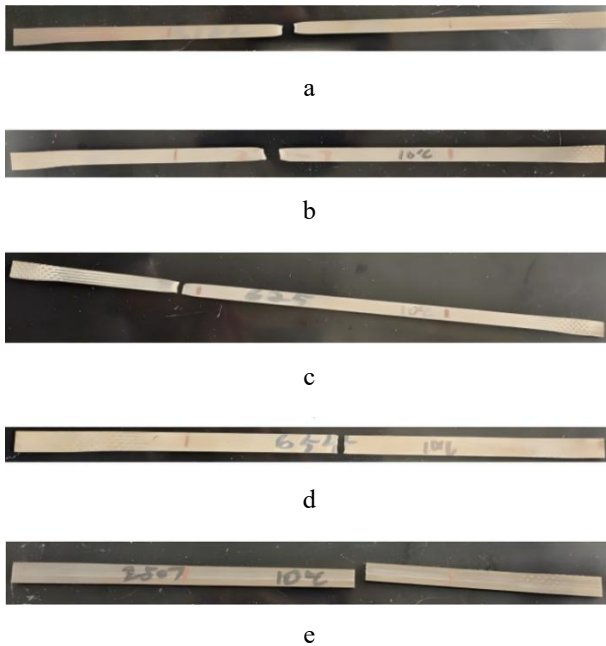


Fig. 4 Sample tensile test results: a – 316L, b – Incoloy 27-7 Mo, c – Incoloy 625, d – 654 SMO, e – 2507

As illustrated in Fig. 4, the five materials exhibit disparate degrees of plastic deformation. Notably, Incoloy 27-7Mo, Incoloy 625, and 316L exhibited pronounced shrinkage and an elevated overall degree of plastic deformation relative to 654SMo and 2507. Table 2 delineates the outcomes of tensile experiments conducted on the aforementioned materials.

As shown in Table 2, the experimental results of these five materials have certain differences from the literature research results. The reasons for this might be the potential differences in the experimental materials and those in the literature (such as heat treatment processes, batches, suppliers, processing histories, etc.), as well as the differences in experimental conditions (such as tensile rates, sample sizes, testing standards, etc.).

As illustrated in Table 2, materials (Incoloy 27-7Mo, Incoloy 625, 316L) that exhibited notable shrinkage at the fracture demonstrated greater bearing face elongation and bearing face shrinkage than those with less plastic deformation (654SMo, 2507).

As illustrated in Fig 5, Incoloy 27-7Mo, Incoloy 625, 316L plasticity and toughness is better; Incoloy 27-7Mo, Incoloy 625, 316L, 654SMo hardening effect is obvious, Hardening effect from high to low: Incoloy 625, Incoloy 27-7Mo, 316L, 654SMo, 2507.

According to the engineering stress-strain curve, it can be seen that 654SMo, 2507 high yield strength, poor plasticity and toughness, belong to the hard and brittle materials; Incoloy 27-7Mo, Incoloy 625, 316L plasticity, toughness, hardening is obvious, but the strength is relatively poor, belong to the soft and tough materials. Based on the above analysis, Incoloy 27-7Mo, Incoloy 625, 316L is recommended as the material of expandable sand screen.

Table 2  
Experimental results of tensile mechanical properties of different materials

Materials	654SMo	Incoloy 27-7Mo	2507	Incoloy 625	316L
Yield strength, MPa	611.7	314.1	638.1	369.1	234.1
Tensile strength, MPa	958.4	694.2	800.2	776.7	558.7
Elastic modulus, GPa	17.909	13.894	18.724	17.597	15.611
Percentage elongation after fracture, %	21.4	50.8	21.7	59.5	60
Percentage reduction of area, %	22.125	48.25	22.125	55.45	58.15
Center point hardness, HRC	38.03	32	32.5	39.9	28.9

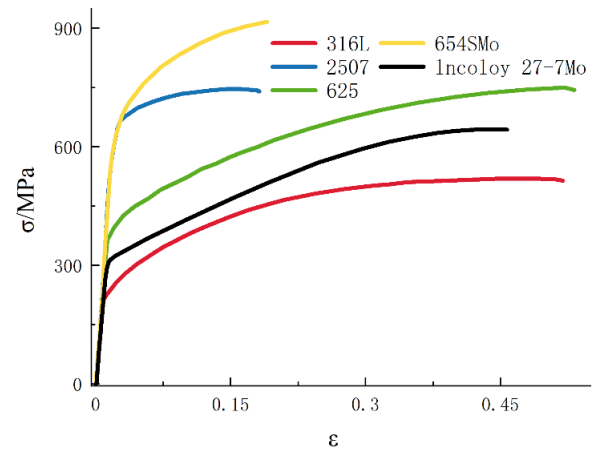


Fig. 5 Engineering stress-strain curves for five materials

### 3.3. Analysis of indoor swelling experiments

The processing dimensions of the simulated expansion test sample are: outer diameter  $\varnothing$  87.8 mm, inner diameter  $\varnothing$  72.2 mm. The expansion rate of the expandable sand screen used in normal construction is generally  $\leq 15\%$ . Considering the increased expansion rate caused by eccentric expansion due to the complex underground conditions, to ensure the successful expansion of the underground expandable sand screen, the designed expansion rate of the screen pipe is  $\geq 17\%$ . Since the outer diameter of the expansion cone used in the expansion experiment is  $\varnothing$  87.2 mm, the expansion rate in the design of the experiment is 17.2%. According to the dimensions shown in Fig 6, the full-scale expansion test specimens were processed. The slotting on the base tube were completed by hydraulic cutting, and the width of all slotting was 1mm. As shown in Fig. 6, the changes in the outer diameter dimensions are recorded at points A, B, C, and D and marked. Fig. 7 shows the sample expansion experiment, through which the expandability of five materials at room temperature is studied.

The results of expansion experiment of prototype with different materials are shown in Fig. 8.

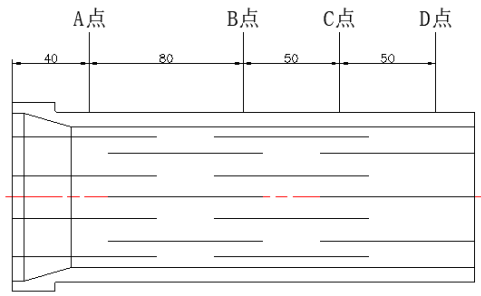


Fig. 6 Expansion experiment sample

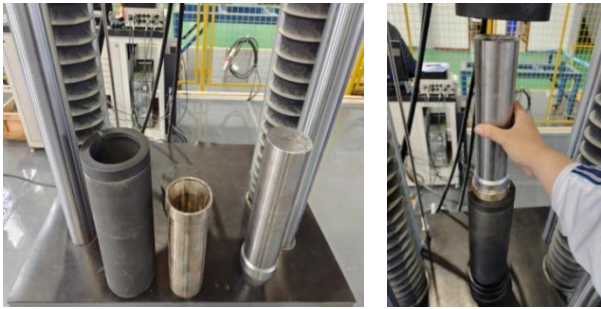


Fig. 7 Sample expansion experiment

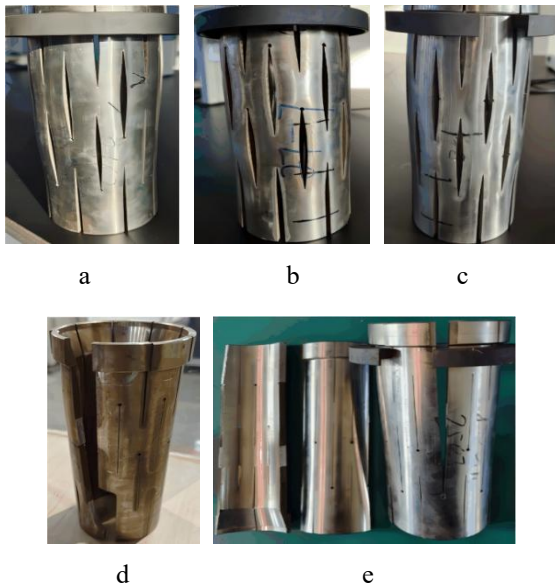


Fig. 8 Results of prototype expansion experiment: a – 316L, b – Incoloy 27-7 Mo, c – Incoloy 625, d – 654 SMO, e – 2507

As illustrated in Fig. 8, the expansion experiment of prototypes of Incoloy 27-7Mo, Incoloy 625, and 316L materials was successful, whereas the expansion experiment of prototypes of 654SMo and 2507 materials was unsuccessful. According to the experimental results of the two materials, 654SMo and 2507, there is no obvious deformation at the kerf of the expandable sand screen, but there is a tearing phenomenon at the butt of the kerf, which indicates that the material has poor plasticity. The prototype of 2507 material exhibited a collapse and cracking into two parts after expansion. Additionally, the prototype of 654SMo demonstrated a taut fracture of the rib during expansion. There was no discernible plastic deformation at the cross-section of the two materials, and the cross-section was relatively flat, indicative of a brittle fracture. This suggests that the material is more brittle. The expansion experiment

of prototype of Incoloy 27-7Mo, Incoloy 625 and 316L materials was successful and no tearing occurred at the butt of kerf. Comparison of the material tensile test results found that the expansion experiment failed in the tensile test results of the performance of the material are not obvious fracture shrinkage, no obvious plastic deformation, are hard and brittle materials.

654SMo and 2507 did not pass the expansion experiment of prototype test, these two materials in the conventional state of the expansion performance cannot meet the requirements of the use of expandable sand screen, such as the use of the annealing process can be used to increase the plasticity of these two materials, in the smaller expansion rate of the working conditions there is a possibility of use.

#### 4. Finite Element Analysis

##### 4.1. Construction and simplification of the finite element model

In consideration of the intricate nature of the down-hole working environment of the expandable sand screen, the following assumptions are made about the model:

1. The issue of defects in the material and processing of the expansion cone and base tube has been overlooked.

2. The influence of stress on the base tube prior to expansion is overlooked.

3. The effect of internal energy consumption and emission due to frictional heat generation during the expansion process is overlooked.

In consideration of the characteristics of the expansion process of the expandable sand screen and the structural characteristics of the expandable sand screen, the structure of the expandable sand screen is simplified. The simplified model and the model division grid are illustrated in Fig. 10. The complete mesh of the model comprises 5528 domain cells, 6652 boundary cells, 1304 edge cells, the minimum finite element size is 0.1 and the average finite element size is 1, and a total of 122706 degrees of freedom for the solution, in addition to 121147,200 internal degrees of freedom. In consideration of the expandable sand screen during the expansion process, the deformation of the expansion cone in relation to the base tube can be disregarded, and the expansion cone is defined as a rigid body.

According to the simplified model structural characteristics and expansion experiments, the model boundary conditions are shown in Fig. 11, setting the axial displacement of the right bearing face of the base tube to 0 mm, setting the axial displacement of the expansion cone, and

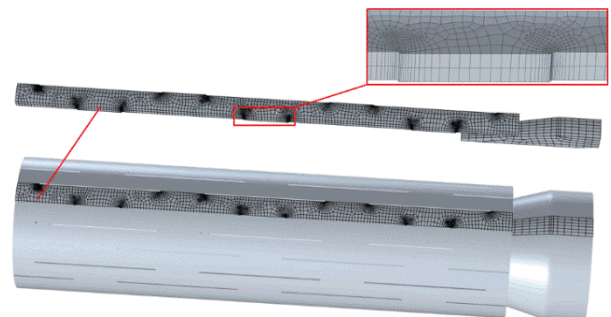


Fig. 9 Simplified model and meshing



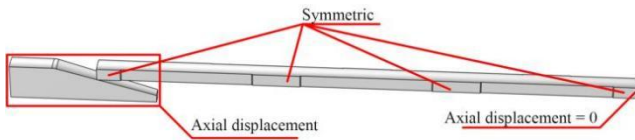


Fig. 10 Boundary conditions

setting the symmetry at the simplified cut surface of the model.

#### 4.2. Material setup

The true stress-strain curves of the five materials are imported into the model, and the material property settings of the five materials are presented in Table 3.

Table 3

Material properties

Materials	E, MPa	Poisson ratio	Yield strength, MPa	Plastic model	Hardening model
654SMo	1.7909E5	0.27	611.7	Large plastic strain	Hardening function
Incoloy 27-7Mo	1.3894E5	0.29	314.1	Large plastic strain	Hardening function
2507	1.8724E5	0.3	638.1	Large plastic strain	Hardening function
Incoloy 625	1.7597E5	0.3	369.1	Large plastic strain	Hardening function
316L	1.5611E5	0.3	234.1	Large plastic strain	Hardening function

#### 4.3. Results of the finite element analysis

As shown in Fig. 11, the results of finite element analysis of 316L are used as an example to analyze the stress distribution characteristics of the base tube after expansion.

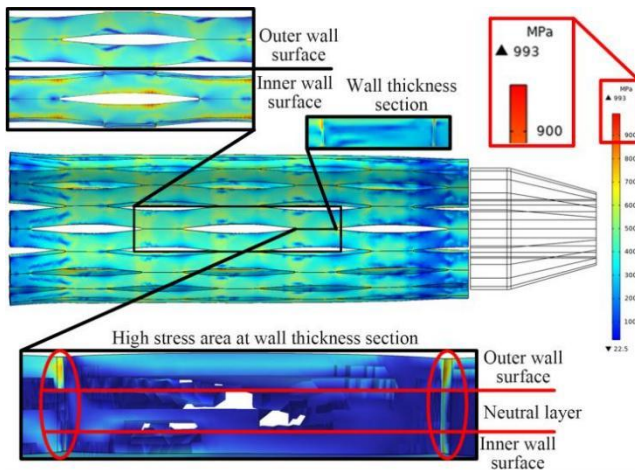


Fig. 11 Results of finite element analysis

As can be seen from Fig. 11, after the completion of the expansion of the expandable sand screen, the obvious stress concentration appeared at the two ends of the bearing face of the kerf, and the stress level of the two sides corresponding to the neighboring kerf was influenced by the stress concentration at the bearing face of the kerf, and the stress was obviously lower than the average stress level of the tube body. Comparison of the stresses on the inner and outer wall surfaces of the base tube shows that the stress distribution on the inner and outer wall surfaces of the base tube is reversed, i.e. the region with a higher relative stress level on the inner wall surface has a lower stress level at the corresponding location on the outer wall surface; and where the stress level on the inner wall surface is low, it is high in the corresponding region on the outer wall surface. The opposite stress distribution on the inner and outer walls of the base tube is due to the fact that the inner wall is mainly subjected to compressive stress and the outer wall is mainly

subjected to tensile stress during the expansion process of the base tube. The stresses in opposite directions on the inner and outer walls are in a state of mutual equilibrium, resulting in the opposite distribution of stresses on the inner and outer walls of the base tube.

The area on the base tube where the stress exceeds the yield strength is defined as the high stress area, and the high stress area of the 316L base tube is 60.2% of the total volume of the base tube, which is recorded as the percentage of the volume of the high stress area. As shown in Fig 12, the high stress region at the wall thickness section, because the stresses in opposite directions on the inner and outer wall surfaces of the base tube are in equilibrium with each other, the expanded base tube is divided into three parts: the outer wall surface, the inner wall surface and the neutral layer. Comparison of the regularity of distribution pattern of the high stress region reveals that the high stress region is much higher than the rest within the stress influence range of the butt of the kerf. This phenomenon indicates that the butt of the kerf will gather a large amount of energy in the process of expansion, and failure will occur when the energy exceeds the material bearing limit. This phenomenon is consistent with crack expansion in fracture mechanics, indicating that the failure form of the expandable sand screen can be analyzed with reference to crack expansion.

### 5. Comparative Analysis

#### 5.1. Comparison of expansion forces

Fig. 12 shows the variation curves of the strain force in the finite element analysis of the five materials.

As can be seen from Fig. 12, the expansion force changes in the process of expandable sand screen are periodic fluctuations. The maximum expansion force of 654SMo is 125990 N, the maximum expansion force of Incoloy 27-7Mo is 74248 N, the maximum expansion force of 2507 is 134620 N, the maximum expansion force of Incoloy 625 is 109,432 N, the maximum expansion force of 316L is 62084 N.

Fig. 13 shows the expansion force variation curve in the expansion test of five materials.

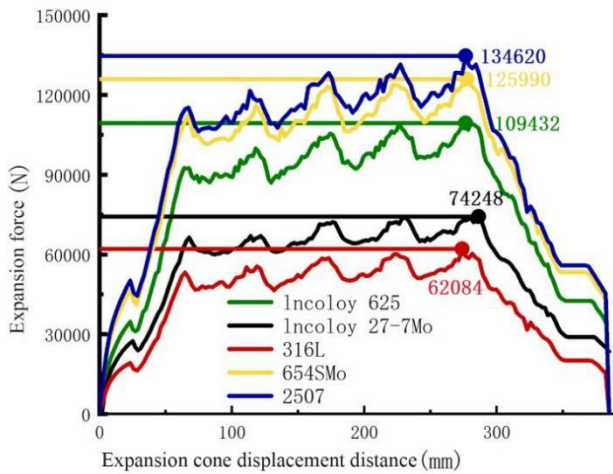


Fig. 12 Finite element expansion force variation curve

As can be seen from Fig 13, Incoloy 27-7Mo, 316L, Incoloy 625 expansion success, 654SMo, 2507 expansion failure. Incoloy 27-7Mo maximum expansion force is 72118 N, the finite element maximum expansion force is 74248 N, the error is 2.9% less than 5%, the error is within the permissible range, the finite element precision meets the requirements. The maximum tensile force of 316L is 59917 N, the maximum tensile force of the finite element is 62084 N, the error is 3.7% less than 5%, the error is within the permissible range, and the finite element accuracy meets the requirements. Incoloy 625 maximum tensile force is 104411 N, the maximum tensile force of the finite element is 109432 N, the error is 4.8% less than 5%, the error is within the permissible range, and the finite element accuracy meets the requirements. Comparison of finite element results and experimental data of Incoloy 27-7Mo, 316L, Incoloy 625 three materials, it is found that the error is less than 5%, the error is within the permissible range, it is possible to simulate and analyze the expansion of the base tube by finite element.

The 654SMo material tears at 85582 N, the tear expands at 91136 N, and the finite element maximum expansion force is 125990 N greater than 85582 N (654SMo tear critical load), so the 654SMo expands and fails. 2507 material tears at 49935 N and the finite element maximum expansion force is 134620 N greater than 49935N (2507 tear critical load), so 2507 expansion fails.

Observation of Fig. 13, a, b, c reveals that the expansion force curves of expandable sand screen with Incoloy 27-7Mo, 316L, and Incoloy 625 as the materials all show more obvious wave peaks, and the overall trend is the same as that of the finite element results. The expansion force curve of the expandable sand screen with 654SMo as the material shows a once cliff-like drop and the overall loading time is short. Comparison of the prototype expansion results showed that the first kerf end of the expandable sand screen showed a tear and the last kerf end showed a taut break, which coincided with the trend of the expansion force curve. It is judged that 654SMo has poorer tear resistance compared to other successfully expanded materials. The expansion force curve of the expanded sand screen with 2507 as the material shows twice cliff-like drops. Comparing the results of the prototype expansion, it is found that a tear at the end of the first kerf of the screen tube causes the loading force to drop sharply, and as the loading proceeds, the tear expands to cause the loading force to drop sharply

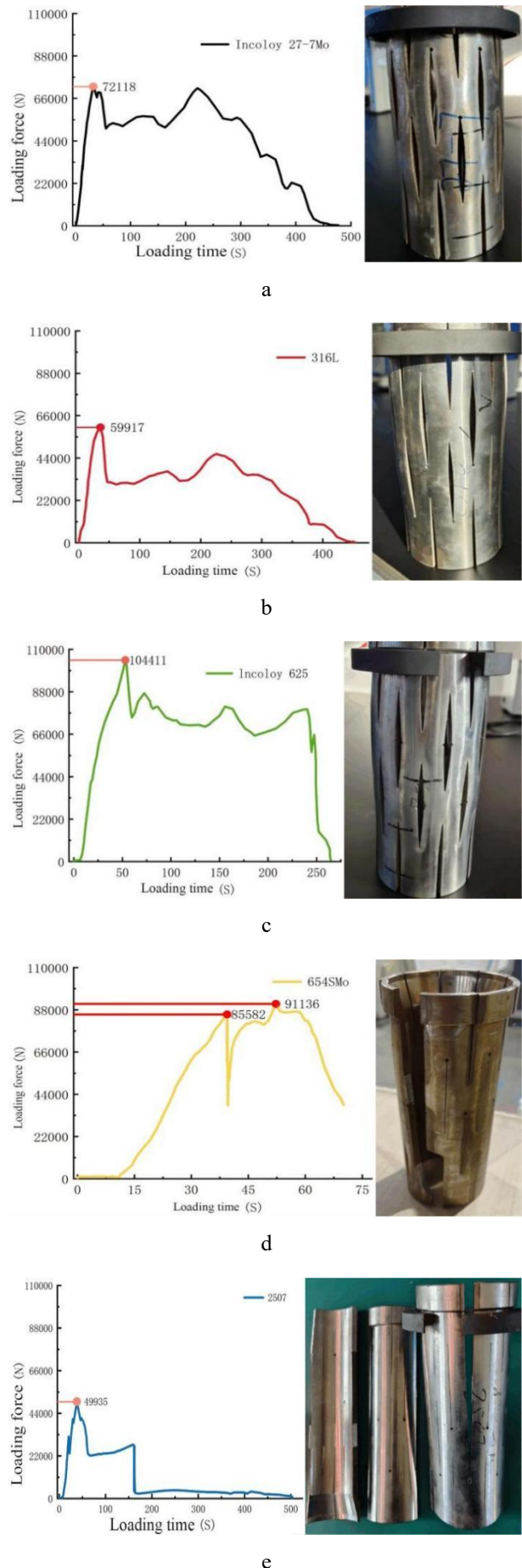


Fig. 13 Expansion experiment expansion force change curve: a – 316L, b – Incoloy 27-7 Mo, c – Incoloy 625, d – 654 S Mo, e – 2507

again, which is consistent with the trend of changes in the expansion force curve. The tear resistance of 2507 material is judged to be poor.

Comparing the experimental results of expansion of the prototype and the experimental results of material stretching, it is found that the expansion of the successful material in the tensile experiment, the fracture surface of the expandable sand screen will be obvious plastic deformation and contraction phenomenon at the same time, and the stress-strain curve of the elastic deformation section is

shorter, the hardening section is longer, and the toughness is better.

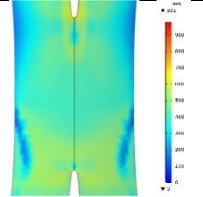
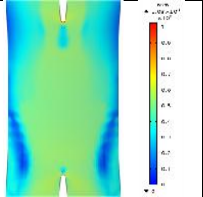
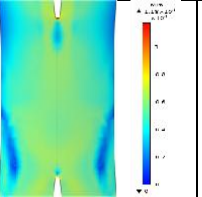
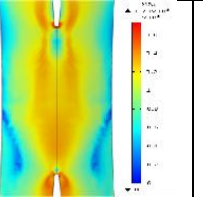
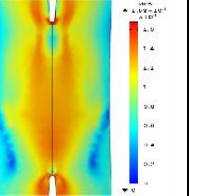
## 5.2. Material variability analysis

The finite element and experimental results for the five materials are shown in Table 4.

From Table 4 it can be seen that the volume percentage of the high stress region is higher for the three materials Incoloy 27-7Mo, 316L and Incoloy 625 than for the

Table 4

Analysis of differences between the five materials

Material	The expansion was successful			Expansion failure	
	316L	incoloy 27-7Mo	Incoloy 625	654SMo	2507
Finite element results					
Volume percentage of high stress area, %	60.2	57.5	48.4	27	27.5
Maximum expansion force, t	6.21	7.42	10.94	12.6	13.46
Stress distribution					
Experimental result					
Yield strength, MPa	234.1	314.1	369.1	611.7	638.1
Elongation, %	60	50.8	59.5	21.4	21.7
Maximum expansion force, kN	59.9	72.1	104.4	Fracture after 100 kN	49.8 kN after fracture
Expansion force error, %	3.7	2.9	4.8		
The average hardness of the tube after expansion, HRC	22.6	26.7	31.8		
Average hardness of slot after expansion	23.2	30.6	38.3		
The hardness of groove is higher than that of pipe body, %	2.59	12.75	17		

two materials 654SMo and 2507. Both materials, 654SMo and 2507, have higher yield strength and tube hardness, lower volume fractions in the high stress areas after expansion (both < 28%) and more pronounced stress concentrations between the bearing faces of the kerf. 654SMo has a lower volume percentage compared to the high stress area of 2507, but higher stress levels between the kerf ends, indicating that the kerf ends collect a lot of energy in a very small area after expansion. When comparing the differences in material toughness, it was analyzed that the better the material toughness, the smaller the volume of the base tube that expands to collect the same energy at the end of the kerf, and the greater the likelihood of the base tube cracking.

Comparing the two materials, 654SMo and 2507, it was found that the finite element analysis showed that the stress level at the end of the 2507 kerf was higher, and the experimental results showed that the 2507 had poorer tear resistance, and the stress-strain curves showed that the 2507 had poorer toughness. The difference between 654SMo and 2507 suggests that the toughness of the material is positively

proportional to the base tube's tear resistance, i.e., a hard and brittle material behaves as if it is prone to cracking in the process of expansion.

Comparing the hardness change, yield strength and elongation of the kerf and tube body for three materials, Incoloy 27-7Mo, 316L and Incoloy 625, it was found that the material yield strength was positively proportional to the hardening effect, the elongation was inversely proportional to the hardening effect and the material yield strength was positively proportional to the maximum expansion force. Combining the data from the experimental results for the five materials, it was found that the risk of breakage of the expandable sand screen during expansion could be analyzed by using the volume percentage of the high stress region as a reference.

According to the results of material testing, expansion testing and finite element analysis, among the three successful expansion materials of Incoloy 27-7Mo, 316L and Incoloy 625, 316L material has low procurement cost and good expansion performance (low expansion force and

high expansion rate), and it can be used as the main material for the base tube. If the anti-corrosion performance of 316L does not meet the requirements, it is recommended to use LNColy 27-7Mo material, which has moderate expansion performance (high expansion force, high expansion rate), excellent hardening effect after expansion, the expansion force is 27.5% higher than that of 316L, and the corresponding mechanical strength of the material is 24.7% higher than that of 316L, which can be adapted to more demanding requirements for deep well use. If there are strict requirements for the corrosion resistance of the material and also higher requirements for the mechanical properties of the material, it is possible to choose Incoloy 625 material.

## 6. Discussion and Recommendations

By comparing the results of the finite element analysis with the experimental results, it was found that the risk of tearing of the expandable sand screen during expansion could be analyzed using the percentage of volume of the high stress region as a reference. The paper has the following shortcomings.

1. According to fracture mechanics, it is possible to measure and prevent the risk of base tube rupture by using the fracture toughness as a reference, but when the conditions of base tube expansion rate, diameter-to-thickness ratio, expansion temperature, etc. are changed, the critical material toughness of base tube rupture corresponding to the conditions will also change, so it is possible to analyze the risk of base tube rupture under different working conditions by using the volume percentage of the high-stress area as a reference.

2. Due to insufficient experimental data, it has not been possible to determine the percentage of volume of the critical high stress region where tearing of the expandable sand screen occurs, and it is necessary to add experimental data to the subsequent study to analyze the critical value at which tearing of the expandable sand screen occurs.

## 7. Conclusions

1. This paper adopts the finite element analysis method combining material tensile experiment and expansion experiment of prototype, and proposes the volume percentage of high stress region as a reference to analyze the risk of tearing in the expansion process of expandable sand screen, and analyses the main material properties affecting the volume percentage of high stress region through the experimental results of the material, which are the yield strength and elongation;

2. Comparison of the finite element results with the experimental results of the expanded sand screen found that the volume percentage of the high-stress region of the expanded sand screen was higher than 48 per cent for all successfully expanded materials. And the hardening effect of the expanded sand screen, the yield limit of the material is inversely proportional to the volume percentage of the high stress region, and positively proportional to the maximum expansion force;

3. According to the research results, under the uncomplex working conditions of conventional oil and gas Wells, that is, for oil and gas Wells with a well depth of 1000-2000 meters and wellbore and formation temperatures lower than 150°C, 316L is more suitable as the base pipe

material. Under unconventional oil and gas well conditions, that is, deep Wells with a depth of 4,000-6,000 meters, a temperature of 120-220°C, a pressure of 60-120 MPa, and oil and gas Wells containing low-concentration corrosive media, Incoloy 27-7Mo is more suitable as the base pipe material. In ultra-deep Wells at 6,000-9,000 meters or extra-deep Wells above 9,000 meters, where the temperature is 150-400°C, the pressure is 120-220MPa, and there are high-concentration corrosive media such as hydrogen sulfide and carbon dioxide, Incoloy 625 is more suitable as the base pipe material.

## References

1. Liu, X. O.; Wang, P. T. 2000. Development and Prospect of Oil Production Engineering Technology, Oil Drilling & Production Technology 22(03): 42-49. <https://doi.org/10.3969/j.issn.1000-7393.2000.03.011>.
2. Han, Z. Y.; Sun, B.; Wang, Y. H.; Cheng, Y. F.; Yan, C. L. 2023. Mechanical Experiments of Deep Sandstone and Sand Production Law in Reservoir Development, Science Technology and Engineering 23(29): 12504-12512. <https://doi.org/10.12404/j.issn.1671-1815.2023.23.29.12504>.
3. Liu, Y.; Wang, Y.; Duan, Y. G.; Zhang, H.; Yang, W. L.; Feng, Q. 2020. Expandable Screen Sand Control Technology in Iran AHWAZ Oilfield, Well Testing 29(03): 50-56. <https://doi.org/10.19680/j.cnki.1004-4388.2020.03.009>.
4. Zhu, H. B. 2012. Research and Application on Base Pipe Material Performance of Expandable Screen, Southwest Petroleum University.
5. Al-Abri, O. S.; Pervez, T.; Al-Maharbi, M. H. 2015. Mechanical and Microstructural Changes of Fine Grained C-Mn Steel Tubular Undergoing Down-Hole Cold Expansion Process, Proceedings of the ASME 2015 International Mechanical Engineering Congress and Exposition Volume 9: Mechanics of Solids, Structures and Fluids. <https://doi.org/10.1115/IMECE2015-51568>.
6. Li, D. J.; Guo, D. S.; Ju, Y. F.; Liang, W. Y.; Zhang, X. T.; Ren, F. Z. 2021. Effect of expansion deformation on mechanical properties and corrosion performance of 20G steel in oilfield produced water, Journal of Materials Heat Treatment 42(06): 115-122. <https://doi.org/10.13289/j.issn.1009-6264.2020-0498>.
7. Zhang, Y. F.; Li, D. J.; Xiong, Y.; Ren, F. Z. 2022. Difference analysis of collapse strength after expansion of two kinds of expandable tubes, Journal of Materials Heat Treatment 43(11): 190-196. <https://doi.org/10.13289/j.issn.1009-6264.2022-0179>.
8. Chen, J. J.; Li, D. J.; Bai, Q.; Lv, N.; Ren, F. Z.; Feng, Y. R.; Song, S. Y.; Liu, Q. 2017. Calculation model of expansion force for expandable tube based on material strain hardening behavior, Journal of Materials Heat Treatment 38(10): 176-183. <http://dx.doi.org/10.13289/j.issn.1009-6264.2017-0233>.
9. Wu, L. G.; Zhu, H. B.; Teng, Z. Z. 2009. Experimental study on expansion performance of expandable slotted pipe, Oil Field Equipment 38(02): 34-38. <https://doi.org/10.3969/j.issn.1001-3482.2009.02.008>.



10. **Zhu, B. F.** 2018. Finite Element Method: Theory and Applications, 4th Edition. Beijing: China Water & Power Press.
11. **Zhao, W. Y.; Sun, G. Y.** 2024. Discussion on Completion Technology of Expandable Screen for Shallow Heavy Oil Thermal Recovery Horizontal Wells, Inner Mongolia Petrochemical Industry 50(8): 65-68.  
<https://doi.org/10.3969/j.issn.1006-7981.2024.08.016>.
12. **Liu, P.; Tang, Z. Q.; Dai, N.; Xiao, Q. L.; Wang, Z. P.; Wang, C. L.** 2023. Study on Mechanical Behavior and Deformation Law of Expansion Process of Expansion Screen Base Pipe, Mechanika 29(5): 350-357.  
<https://doi.org/10.5755/j02.mech.33414>.

X. Wu, J. Lin, H. Tian, W. Yang, Y. Wang

#### ANALYSIS OF MATERIAL OPTIMIZATION AND PERFORMANCE PARAMETER DIFFERENCE OF EXPANDABLE SAND SCREEN

#### S u m m a r y

Sand control technology of expansion sand screen is one of the effective methods to solve the sand problem in oil wells, due to its unique working mode, which has significant benefits in improving production and reducing costs, and has been widely used in the oilfield field. However, the operational conditions that expansion sand screens are subjected to, such as high temperatures, high pressure and high corrosion, exert greater demands on the material performance of the expansion sand screens. The advancement of this technology is predominantly constrained by the intrinsic characteristics of the material in question. In this study,

five materials were selected as the base tube materials of the expansion sand screen, namely stainless steel 654SMo, stainless steel Incoloy 27-7Mo, stainless steel 2507, stainless steel Incoloy 625 and stainless steel 316L. These materials were chosen based on their performance requirements in relation to the expansion sand screen. The impact of diverse materials on the expansion performance of base tubes was investigated through a multifaceted approach, integrating tensile experiments, prototype expansion experiments, and finite element analysis. The experimental results demonstrate that stainless steel 316L is a more suitable base tube material under the condition of relatively low requirements for temperature and corrosive environment. Conversely, stainless steel Incoloy 27-7Mo is a more suitable base tube material in more demanding deep well environments. Finally, stainless steel Incoloy 625 is a more suitable base tube material for working conditions with higher requirements for corrosion resistance and mechanical properties. A comparison of the results of the finite element analysis with those of the prototype expansion experiment indicates that the volume percentage of the high stress region is a useful indicator of the expansibility of the base tube to a certain extent. The findings of this study provide a novel evaluation metric for the optimization of parameters and the selection of materials for expandable sand screen. This has the potential to reduce costs and time during the research process.

**Keywords:** expandable sand screen, difference analysis, material optimization, finite element analysis.

Received December 1, 2024  
Accepted June 25, 2025



This article is an Open Access article distributed under the terms and conditions of the Creative Commons Attribution 4.0 (CC BY 4.0) License (<http://creativecommons.org/licenses/by/4.0/>).